Universitat Autònoma de Barcelona

Dipòsit digital de documents de la UAB

This is the **submitted version** of the article:

Alam, Saiful; Shabik, Fazle; Rahman, Mohammed M.; [et al.]. «Enhanced electrocatalytic effects of Pd particles immobilized on GC surface on the nitrite oxidation reactions». Journal of Electroanalytical Chemistry, Vol. 839 (April 2019), p. 1-8. 8 pàg. DOI 10.1016/j.jelechem.2019.02.058

This version is available at https://ddd.uab.cat/record/255121

under the terms of the BY-NC-ND license

Elecetrocatalytic oxidation of Nitrite ions using Pt-Pd bimetallic electrode

Md. Saiful Alam [a], Md. Fazle Shabik [a], M.M. Rahman [b], Manel del Valle [c], Mohammad A. Hasnat[a, *]

[a] *Department of Chemistry, School of Physical Sciences, Shahjalal University of Science and Technology, Sylhet 3100, Bangladesh*
[b] *Center of Excellence for Advanced Materials Research (CEAMR) and Chemistry Department, Faculty of Science, King Abdulaziz University, P.O. Box 80203, Jeddah, 21589, Saudi Arabia*
[c] *Grup de Sensors i Biosensors, Departament de Quimica - Quimica Analitica, Universitat Autonoma de Barcelona, Edifici Cn, Campus de la UAB, 08193 Bellaterra, Barcelona, Spain*

Abstract

In the present paper, nitrite oxidation reaction has been performed using a pristine GC and Pd modified glassy carbon (GC) electrode to investigate catalysis and kinetics of nitrite (NO_2^-) oxidation reactions. The performance of GC electrode increased towards the nitrite oxidation reaction when it achieved catalytic influence from Pd particles. The NOR over the Pd-GC electrode followed by two steps process where the charge transfer steps coupled with the chemical reaction. The nitrite ions involve a single electron transfer reaction NO_2 being the product, which later undergo through a dispropornation reaction yielding NO_2^- and NO_3^- as final products.

1.1. Introduction

Inorganic substance nitrite (NO_2^-) is a toxic contaminant that inflicts threat towards drinking water, food and so on. The permissible level to uptake NO_2^- ion is < 8 mg for an adult suggested by the World Health Organization [1, 2]. Highly exposure of NO_2^- contains the greatest health risk particularly for pregnant women even for infants [3]. Methemoglobin resulted from the nitrite byproduct can damage the oxygen cells in human body generally seen in case of pregnant women [4, 5]. However, bearing positive sides including as meat preservatives, coloring agent, enhancing the artificial flavor nitrite largely use in the worldwide disregarding the detrimental sites [6]. Therefore, measurement of NO_2^- analytically and the behavior study of NO_2^- are more significant to the researcher. Some analytical techniques are generally used to monitor the nitrite behavior like spectrophotometry [7, 8], fluorescence [9, 10], liquid chromatography [11–13], capillary electrophoresis [14, 15], and chemical luminescence [16]. The unfriendly nature of these techniques such as time-consuming process, less cost effectivity, sensitivity, efficiency and response time covers these systems are more complex for specific analysis [17]. In contrast, because of the high sensitivity with more precession, no complexity in uses, rapid response makes the electrochemical technique more preferable to perform [18]. Therefore, the electrochemical study of NO_2^- is more reliable and well documented in the literature [19]. However, the electrochemical behavior of nitrite over pure solid electrode is more conventional and intricate to study due to the easily surface contamination need more activation energy or overpotential to exhibit its performance [18]. With the aim of reducing the required overpotential, influence of interference and enhancement of sensitivity it is essential to amplify the active surface area that can be achieved by the surface modification [20]. The modified electrode may influence the electrode kinetics, effective surface area and diffusion regime [21] results the altering at signal magnitude and overpotenital. In order to electrode modification, various types of materials have been used including polymeric films and metal nanoparticles. Most of the time some metals and bimetallic nanoparticles exhibits the amazing catalytic behavior such as Au, Pt, Pd, Fe, Cu, Sn, Ag [22-26]. However, deposition of nanoparticle on pure solid electrode play a great role in case of electrochemical analysis (response, kinetics and mechanism) of nitrite oxidation reaction (NOR) [27-29]. In this present article, we mainly focused on the Palladium (Pd) nanoparticles as modified material on Glassy carbon (GC) electrode to fabricate the Pd-GC electrode. GC is an electrode

having very sluggish electron transfer kinetics largely found in inner sphere process. The interference of oxygen and other analytes circumvent the analysis require high overpotential. Additionally the adsorption of species on the electrode surface is not smooth well [34/30]. Therefore, the modification of GC electrode is essential to avoid the above sophisticated problems. Realizing this we were much more concentrated on the Pd material to assemble the bimetallic (Pd-GC) electrode for the NOR. Pd has some smart properties that induced to consider it like versatility, cost-effective, containing non-toxic properties, high electro-catalytic activity and having more resistance to exhibit the oxygen presence as well as moisture [31]. Previously using Only Pd as modified material in order to nitrite analysis was not well assessed but as composite material Pd was addressed by some authors. For example, Jing-He Yang et al reported the activity of the graphite supported Pd (Pd/Grp) nanocomposite modified GC electrode on NOR where the Pd/Grp imposed its catalytic property on GC electrode resulting the best sensitivity to detect the nitrite ion rather than the bare GC electrode **[31]. Ya Zhang also used Pd containing composite** on GC electrode to boost the electrocatalytic property in nitrite detection and found excellent catalytic property with high sensitivity [32]. Various papers has been published to establish the Pd containing electrode as sensor to sense the nitrite ion but less attention has been put on the analysis of the electro-kinetics of corresponding reaction. In this paper, mainly we discussed the catalytic activity of Pd on GC electrode towards the nitrite oxidation reaction, mechanism of this oxidation process and lastly the related kinetics has been measured. The deals of catalytic activity, mechanistic aspects and electro-kinetics of the nitrite oxidation reaction has been accomplished via cyclic voltammetric techniques (CVs), Hydrodynamic voltammetric techniques using rotating disk electrode (RDE).

2. Experimental

The required chemicals were sodium nitrite ($NaNO_2$), potassium chloride (KCl), hydrochloric acid (37%), Sodium phosphate monobasic dehydrate, sodium phosphate dibasic were purchased from Sigma-Aldrich and used without further purification. Mili-Q-Water resistivity less than 18 MΩ cm^{-1} was used to prepare all solutions. Electrochemical experiments such as cyclic and hydrodynamic voltammetric have been carried out by Autolab potentiostat (PGSTST 128N, The Netherlands) a conventional three-electrode cell. A GC disk electrode having 2mm diameter coated with Teflon jacket was chosen as working electrode whereas Ag/AgCl (saturated KCl) was

reference and a Pt wire electrode was counter electrode. As part of GC electrode cleaning firstly the electrode surface was rubbed using alumina (0.3mm) slurry on a soft lapping pad until a mirror like shiny surface then sonicated with 0.05 M H_2SO_4 for 15 mins at 28^0C.

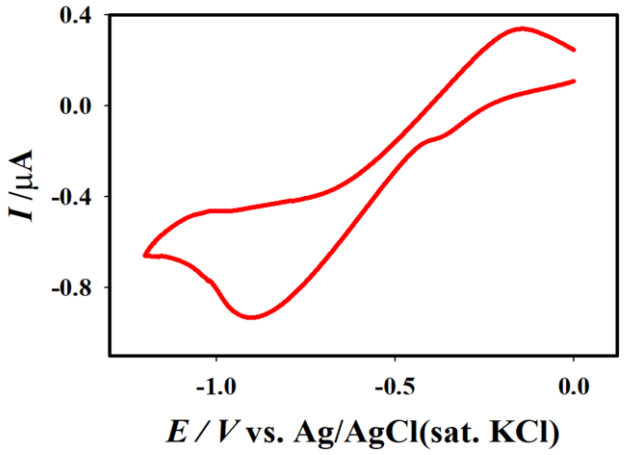

Fig. 1. CV of Pd deposition on GC from N_2 saturated 0.1 M $PdCl_2$

GC electrode surface was cleaned voltammetrically by cycling the potential in 0.1M H_2SO_4 repeatedly within the potential window -0.2V to 1.5V at a scan rate of 100 mV s^{-1} until the characteristic cyclic voltammogram of GC cleaning was obtained. The deposition of Pd particle from N_2 saturated 0.1 M $PdCl_2$ solution on GC electrode was treated through electrochemically on cleaned GC surface by recording the CVs scan in the range of potential from 0.0 to -1.0 V at a scan rate of 0.1 Vs^{-1} for 10 cycles and the deposition curve is shown in Fig 1.

For electro-oxidation of NO_2^- the GC electrode along with counter and reference electrodes were placed in a three-electrode cell which contain the analyte 10 mM $NaNO_2$ in 0.1 M KCl. Bulk electrolysis was performed using a conventional cell. In order to study the surface morphology of Pd deposited GC electrode Leo Supra 50 VP scanning electron microscope (SEM) was used whereas for the elemental analysis on Pd-GC electrode surface Oxford INCA 400 energy dispersive X-ray spectroscope (EDX) was used.

3. Results and discussion

3.1. Surface analysis

Figure 2. shows the FE-SEM image of Pd particles deposited on GC surface along with corresponding EDS spectra. From the FE-SEM (25,000 X), it is seen that Pd particles are globular in shapes over the GC surface. The EDS spectra reveals that only Pd particles were deposited on the GC surface without any impurity. However, in order to understand the properties of the catalytic surface XPS analysis of the surface was performed as shown in Fig. 3. Pure Pd particles exhibits doublets as reported in literature, the binding energy of metallic Pd(0) for $3d_{5/2}$ is 335.3 eV and for $3d_{3/2}$ is 340.71 [33].However, the XPS spectra of Pd particles over GC surface yielded doublets from spin-orbital splitting of the $3d_{5/2}$ and $3d_{3/2}$ states centered at 335.4 eV and 340.7 eV, respectively. Along with the doublets, an additional shoulder like peak (BE= 337.5 eV) was also appeared, which is may be attributed for the existence of Pd^{2+}. It is worthwhile to note that Pd^{2+} (BE= 337.5 eV) has higher binding energy than reported binding energy of Pd^{2+} at 336.9 eV [34]. Thus the difference in BE for the peaks of deposited Pd particles from the literature value, one can assume that Pd particles have a strong interactions with GC surface. This observation suggests that a Pd-GC surface should be catalytically different from that of a pure Pd surface.

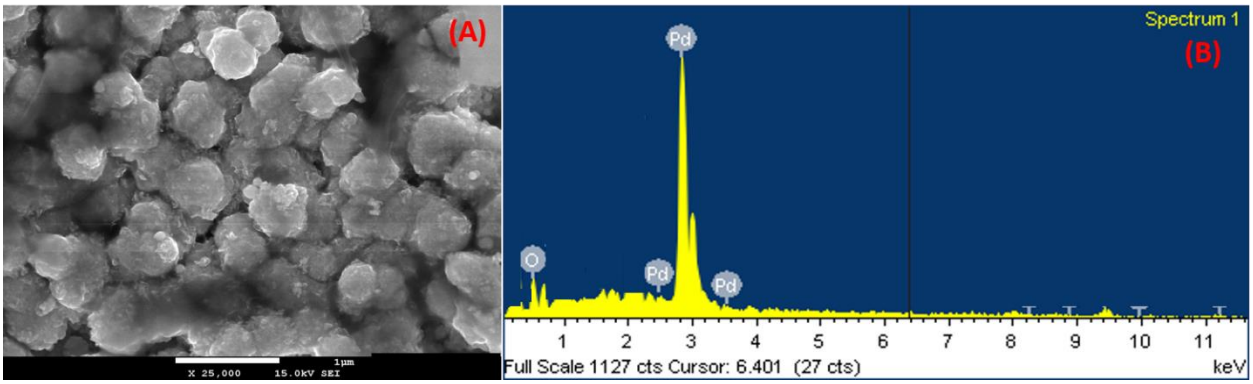

Fig. 2. FE-SEM image of Pd particles on GC (A) and associated EDS spectrum (B).

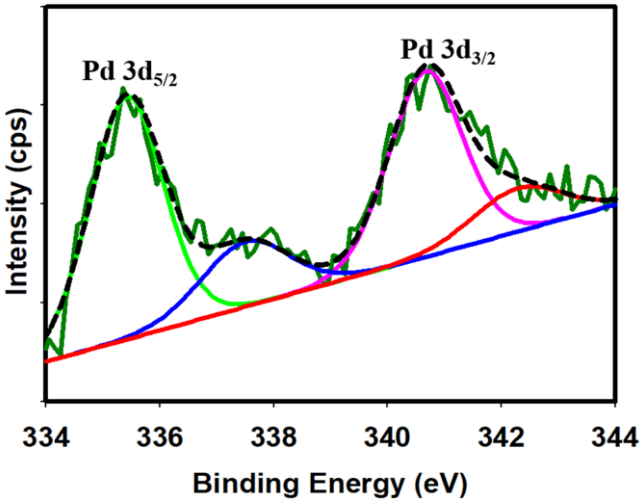

Fig. 3. XPS fine scan spectra for Pd 3d of the deposition of Pd over GC

3.2. Catalysis

Figure 4. Shows the typical cyclic voltammograms (CVs) of N_2 saturated 10 mM $NaNO_2$ in 0.1M KCl solution recorded by three different electrodes such as GC, Pd-GC, and Pd at a fixed scan rate of 50 mVs^{-1}.

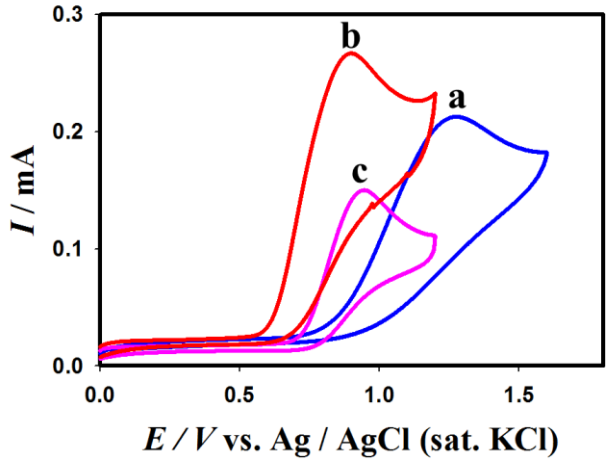

Fig.4. Cyclic voltammograms of 10 mM $NaNO_2$ in 0.1M KCl recorded at a scan rate of 0.05 Vs^{-1} using (a) GC (b) Pd_GC (c) Pd under N_2 saturated condition.

In each case, single anodic waves are observed notifying that nitrite ions undergo oxidation reactions under the experimental condition.

Table 1 Voltammetric properties of different electrodes with respect to NOR

Electrode	Ei/ V	Ep/V	Ip/ mA
Pd	0.75	0.90	0.15
GC	0.81	1.26	0.21
Pd-GC	0.55	0.84	0.29

Note: All the experimental conditions are same mentioned in Fig.4, Ei is the starting potential of Faradic process.

Several voltammetric data pertaining to NOR obtained by using Pd, GC and Pd-GC electrodes are tabulated in Table 1. Among the three electrodes, the Pd electrode exhibited least activity toward NOR as it shows least diffusion current (0.15 mA at Ep of 0.90 V) originated due to NOR. Meanwhile, a GC electrode exhibits a NOR peak current of 0.21 mA at 1.26 V which is larger than that exhibited by a Pd electrode. However, while Pd particles were immobilized on a GC surface, synergistic effects were seen as the GC-Pd electrode exhibited maximum NOR current (0.29 mA) at a minimum potential value of 0.84V. Additionally staring potential of Faradic process (Ei) concerning NOR was appeared at 0.75, 0.81 and 0.55V for Pd, GC and Pd-GC electrodes, respectively. These observations suggest that faster electron transfer and maximum catalytic sites can be obtained by a GC-Pd electrode. Thus, a GC-Pd electrode may be employed to obtain nitrite reduction reactions. As this electrode is noble in attaining NOR, steps were taken next to unveil the reaction kinetics.

3.3. Kinetics

While nitrite ions are scanned from a starting potential of 0.0 V using a GC-Pd electrode, an oxidation wave is seen to appear at 0.84V due to oxidation of nitrite ions as shown in Fig.4. As the oxidation number on N (of NO_2^-) is +3, one can assume that any of the following reactions probably took **place [35-38].**

Route 1.

$$NO_2^- + H_2O \rightarrow NO_3^- + 2H^+ + 2e^- \quad (1)$$

Route 2.

$$NO_2^- \rightleftarrows NO_2 + e^- \quad (2)$$

The number of electron transfer make the basic difference between route 1 & 2. Having two electrons transfer route (1) follows the single step reaction whereas the route (2) involves a single electron transfer process where NO_2 might be the product. The reaction pathway is highly depends on the reaction medium, properties of electrodes materials, temperature as well as the pH. The electrode nature mainly drive the reaction route by executing the surface reaction via formation of oxide layer which influences the reaction kinetics [35, 36].

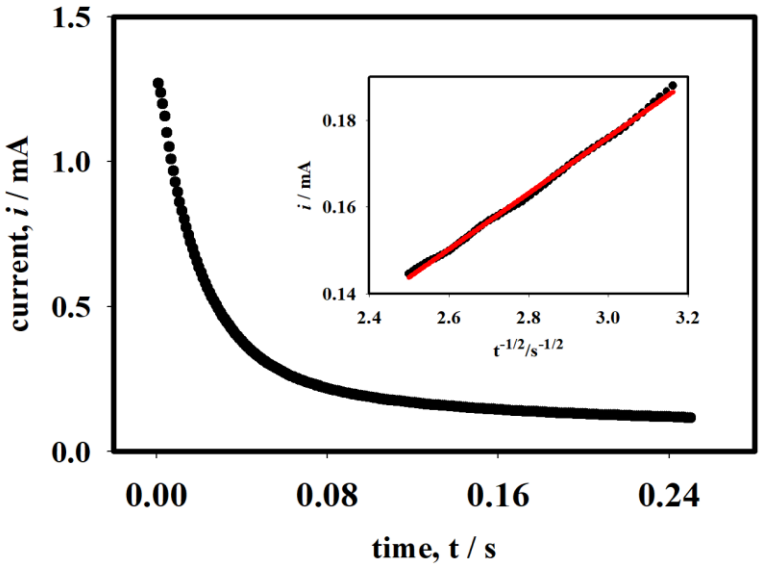

Fig. 5. Chronoamperogram of 3 mM $NaNO_2^-$ at Pd-GC electrode. Inset shows the linear relationship between square root of time and current. Working potential was 0.57 V.

In order to identify the number of electron transfer, in the present case, chronoamperometric technique was used where the recorded chronoamperograms were obtained with respect to 3mM NO_2^- in 0.1M KCl. Here, the chronoamperograms were recorded by stepping the working potential by 20 mV from 0.53 V to 1.2 V. It was observed that the data received from between 0.57 V and 1.0 V matched well with the Cottrell equation (1) [39] and a corresponding chronoamperogram recorded at 0.57 V is displayed in Fig. 5.

$$I = \frac{nFAC\sqrt{D}}{\sqrt{(\pi t)}} \quad (3)$$

Where, I = current (A), n = number of electrons involved in the electron transfer reaction, A = area of the electrode in cm^2. C = concentration of analyte in mol cm^{-3}, D = diffusion coeficient expressed as cm^2/s (2×10^{-5} cm^2/s), t = time in second.

The slope of I vs $t^{-1/2}$ plot (inset Fig. 5.) was used to determine the electron number involved in NOR which was estimated to be 1.15 indicating that only single electron perhaps participated in the charge transfer reaction. This observation entails us that route (2) probably involved on the surface of GC-Pd electrode under the experimental condition by generating NO_2 as product. To justify this observation, 120 min long bulk electrolysis experiment was carried out where the initial concentration of NO_2^- was 0.9 mol/L.

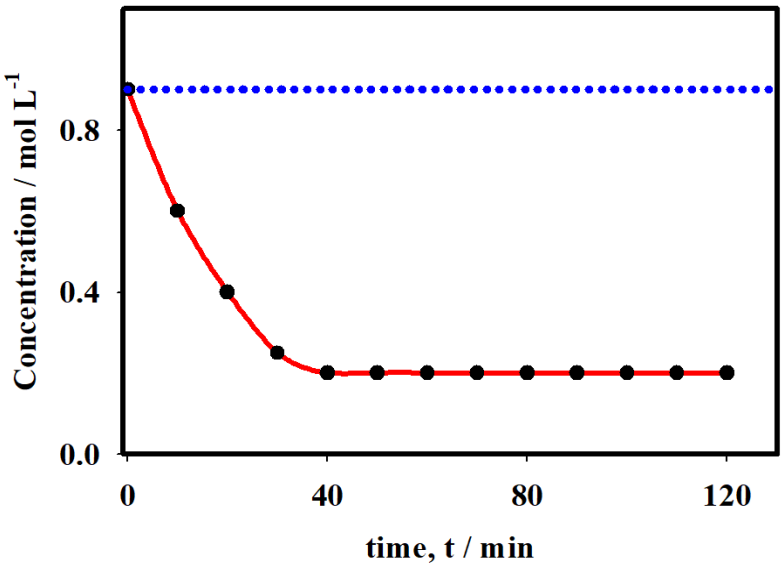

Fig. 6. Bulk electrolysis profile of N_2 saturated 0.9 M $NaNO_2$ in 0.1 M KCl

Using an ion selective electrode total concentration of NO_2^- and NO_3^-(TN) was determined by collecting samples using syringe just from near the electrode surface at different time intervals . It can be seen from Fig. 6 that , the value of TN decreased rapidly and reached to a plateau after 40 min where the value of TN was 0.21 mol/L. If NO_3^- was the only product generated due to electrolysis then the TN would remain constant. By estimating the mass balance, it is observed that 76.6% mass was lost which means that at the electrode-solution interface NO_2^- ions were not directly converted into NO_3^- rather some gaseous molecules were generated. Thus the only possible

product is NO_2 molecules which generated via route (2). However, several previous researches have revealed that NO_2 molecules in water is not stable and undergo dispropornation reaction as per following reaction [35-38].

$$NO_2 + H_2O \rightarrow NO_2^- + NO_3^- + 2H^+ \quad (4)$$

Dependency of scan rate often reveals important kinetic information, hence LSV of 10 mM $NaNO_2$ in 0.1 M KCl at different scan rate ranging from 20 mVs^{-1} to 200 mVs^{-1} as shown in Figure 7.

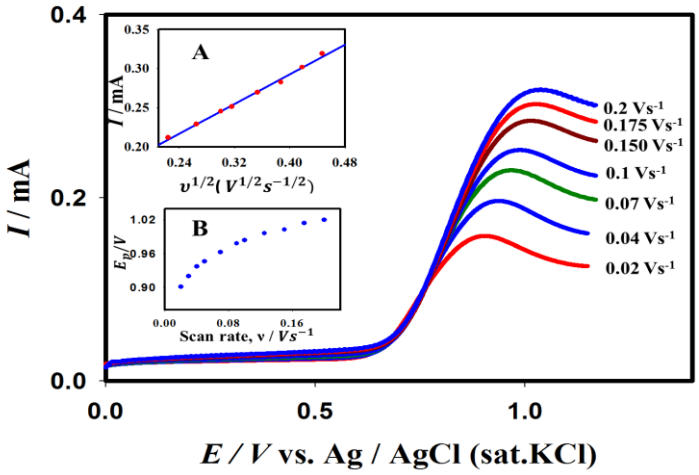

Fig 7. Scan rate dependent LSVs obtained in 10mM $NaNO_2$ in 0.1M KCl and inset (A) shows the relationship between the peak current (I_p) vs square root of scan rate ($\upsilon^{1/2}$). The solid line indicates the regression line. Inset (B) represents the E_p variation with the change in scan rate in a range of 0.02 Vs^{-1} to 0.2 Vs^{-1}.

The I_p value shifted to higher values as the scan rate was increased as shown in Fig. 7. The linear relationship of I_p vs $\upsilon^{1/2}$ (inset A of Fig. 7.) suggests that NOR is a diffusion controlled and shifting of E_p towards higher potentials with respect to the scan rate (inset B of Fig. 7.) indicates that the process is irreversible [40,41]. Note that the magnitude of difference between peak potential and half peak potential was found to vary between 178 mV – 220 mV, and slope of E_p vs. logυ (Fig. 8.) plot was equal to 109 mV. This observation entails us that the electron transfer determined the NOR process on the GC-Pd surface in the neutral medium [42]. Based on this analysis we can assume that the first step is not only the electron transfer but also the rate-

determining step. For further analysis of rate determining step, we have evaluated the transfer coeffiecnt (β) value from the peak potential and half peak potential difference using the equation (5) & (6)[40-42]

$$\beta = \frac{1.86RT}{F|E_p - E_{p/2}|} \quad (5)$$

$$\beta = \frac{-RT}{F(\partial E_p/\partial log\upsilon)} \quad (6)$$

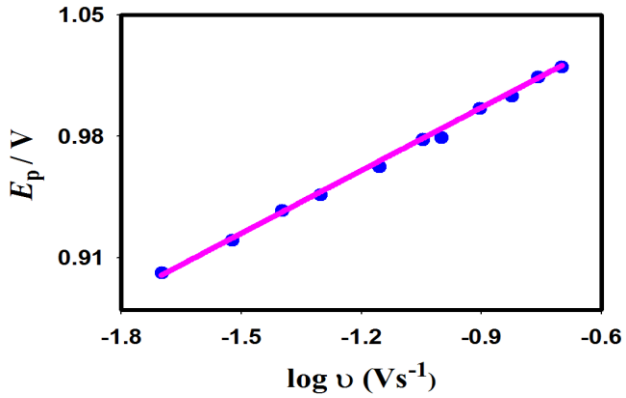

Fig. 8. Peak potential vs log of scan rate of 10mM $NaNO_2$ in 0.1M KCl on Pd-GC electrode.

Using equation (5) and (6) the value of β was found in the range of 0.22-0.26 while the scan rate rises from 20 mVs^{-1} to 200mVs^{-1}. The small value of β (<0.5) provides two significant mechanistic information; the NOR was not only controlled by slow electron transfer step but also a chemical step was concerted [42]. In our cases, this assumption well matched with route 2 considering the mechanistic aspects.

3.4. Heterogeneous Electrokinetics

As the transfer coefficient remained almost constant at variable scan rates, it was then possible to take advantage of RDE data to interpret the kinetic parameters of the NOR process [39].

Fig. 9. Shows the hydrodynamic voltammograms of 10 mM $NaNO_2$ in 0.1 M KCl solution in neutral media obtained by Pd-GC electrode at different electrode rotation rate in the range of 100-3000 rpm with a specific scan rate 0.05 Vs^{-1}.

Like cyclic voltammetric measurements, the nitrite oxidation reaction in the hydrodynamic measurement started at 0.0V and well-defined sigmoidal shaped voltammograms were obtained at all rotation rates. The limiting current density (J_L) began at E < 1.1 V at 100 rpm that shifted slightly with the increase of rotation rates. Conversely, the J_L was found at 1.3 V and moved a slightly towards positive direction due to diffusive nature of electron transfer process.

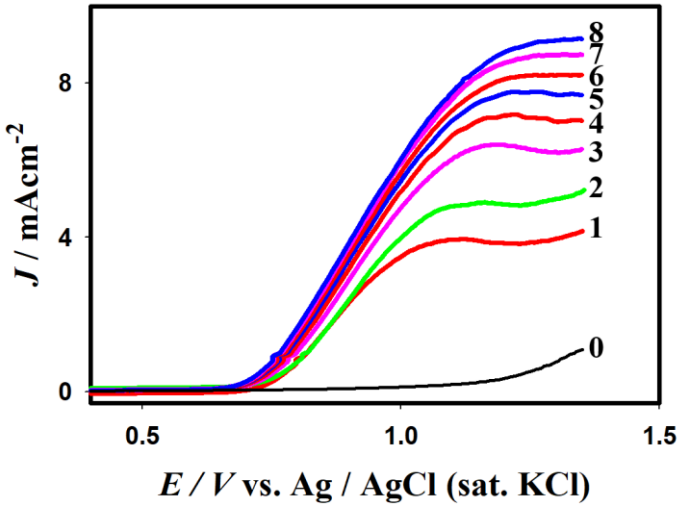

Fig. 9. Hydrodynamic voltammograms recorded at Pd-GC electrode containg 1.0 mM $NaNO_2^-$ in 0.1 M KCl. Rotation rates are: (0) background, (1) 100, (2) 200 (3) 750, (4) 1250, (5) 1500, (6) 1750, (7) 2000, (8) 2500, (9) 3000 rpm. These data was taken at 0.05 Vs^{-1}.

3.5. Limiting current density

The limiting current density for NOR can be defined by equation (7) known as Levich equation **[43-45]**

$$i_L = 0.62\, nFAC_b D_0^{2/3} \upsilon^{-1/6} \omega^{1/2} \qquad (7)$$

Where n is the number of electron that participated in this oxidation reaction, F is the Faraday constant (96500 C), A is the geometric surface area of RDE electrode, C_b is the bulk concentration of $NaNO_2$ (9×10^{-3} mole dm^{-3}), D_0 is the diffusion coefficient value of NO_2^- (2×10^{-5} $cm^{-2}s^{-1}$) [36], υ is the kinematic viscosity and ω is the angular rotation rate that can be defined by $\omega = 2\pi f/60$,

where *f* is the rotation per minute. Using the value of J_L in Levich equation (11) we also verified the possible number of electrons involved in this oxidation process.

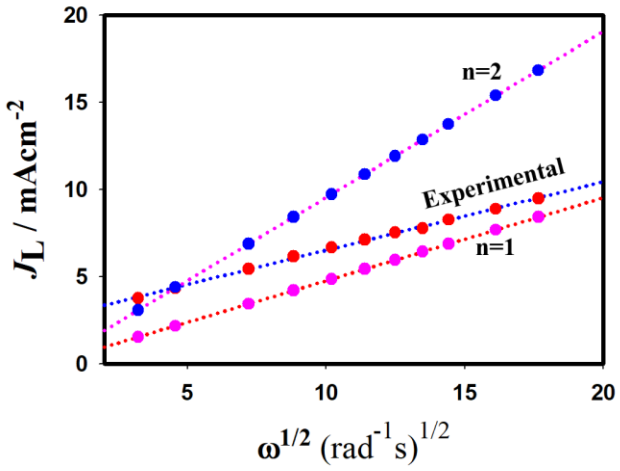

Fig. 10. Levich plot for the nitrite oxidation reaction of 10mM $NaNO_2$ solution in 0.1 M KCl at the Pd-GC electrode. The limiting current density (J_L) were obtained from Fig. 9.

The equation (7) gives a linear relationship between J_L and $\omega^{1/2}$ with a slope value equal to the number of electrons exchanged per NO_2^- ion in the overall anodic reaction. The Plot of experimental values of J_L vs $\omega^{1/2}$ provided a straight line as experimental line with the slope value 0.393 mA cm^{-2} (rad s^{-1})$^{-1/2}$ indicated blue dotted line in the graph suggested that the reaction of nitrite oxidation is controlled by diffusion of NO_2^- to the Pd-GC electrode surface. The J_L values also estimated based on the equation (7) by putting *n*=1 & 2 with respect to the all square root of rotation rates and also found the straight line as theatrical line indicated by pink and red dotted lines. The obtained slope value were 0.476 mA cm^{-2} (rad s^{-1})$^{-1/2}$ and 0.971 mA cm^{-2} (rad s^{-1})$^{-1/2}$ for *n*=1 and *n*=2 respectively. From this analysis it has been found that the obtained slope for *n*=1 had consistency with the slope value obtained by the experimental value that suggested this oxidation reaction occurred by one electron transfer which was well matched with the chronoamperometric measurement.

3.6. Reaction order determination

The reaction order with respect to the dissolved NO_2^- was measured by varying the electrode rotation rate using the following equation (8) [43-45]

$$\log(j) = logj_k + mlog(1 - (j/j_l) \quad (8)$$

Where j_k is the kinetic current density, j is the disk current density, m is the reaction order for NO_2^- oxidation and j_L is the limiting current density.

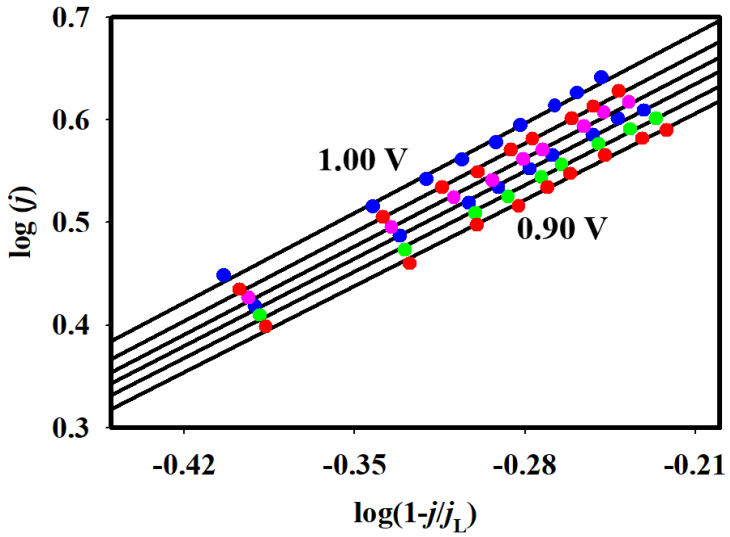

Fig. 11. Linear plot of log (j) vs log (1-j/j_L) at specified potential: (a) 0.90, (b) 0.92, (c) 0.94, (d) 0.96, (e) 0.98 and (f) 1.00 V taken by Pd-GC electrode in 10 mM $NaNO_2$ solution. The data were derived using **Fig. 9.**

Equation (8) can be suitable in the case of activation-diffusion control reaction. The j values were derived from the kinetic region of Fig. 8. at different potential in the range of 0.90 V to 1.00 V where the j_L was obtained at 1.3V. However, using the obtained values of j and j_L, the linear plot of log (j) vs. log (1-j/j_L) was found (**Fig 11)** with the slope values between 1.15 to 1.20 suggested that the corresponding heterogeneous charge transfer reaction of NOR at Pd-GC followed a first order kinetics. At < 0.78V the nitrite oxidation was not significantly influenced under the diffusion of NO_2^- ions. Therefore, this above method cannot be implied at the potential less than 0.78 V.

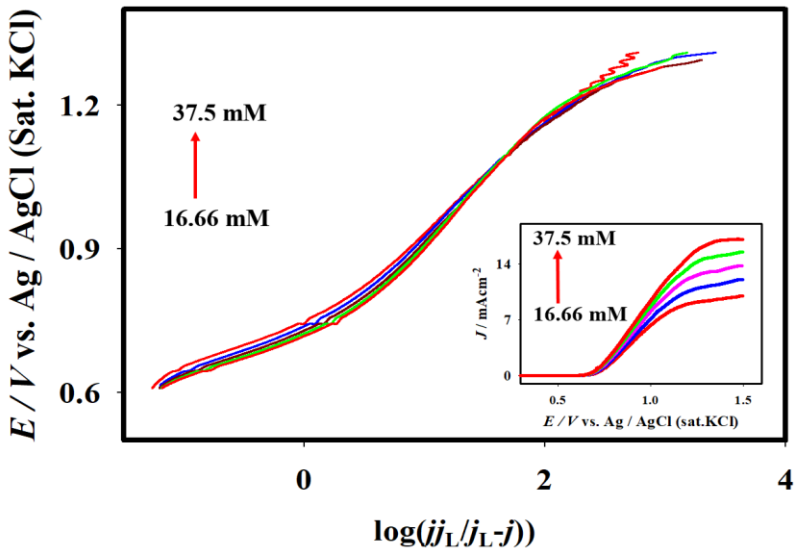

Fig. 12. Polarization curves recorded in tafel form by Pd-GC electrode for (a) 16.66, (b)23.06, (c)28.57, (d) 33.33, (e) 37.50 mM $NaNO_2$. Inset shows the hydrodynamic voltammograms obtained by Pd-GC electrode at this given concentration. Experiment was performed at 500 rpm and 0.05 Vs^{-1}.

In such circumstance, the reaction order can be determined by varying the NO_2^- concentration in the solution. Regarding this issue, the hydrodynamic voltammograms (inset of Fig 11.) were recorded for different concentration of NO_2^- in 0.1M KCl solution over the Pd-GC electrode and results are depicted as Tafel plots in Fig 12. Here, the reaction order with respect to the NO_2^- concentration is determined by plotting corrected kinetic current evaluated according to equation (9)[45] for diffusion effect against the different concentrations of NO_2^- ion at various particular potential from 0.72 V to 0.85 V. The slope values of such plot (Fig 13.) on given potential range varied from 1.15 to 1.18 had a reasonable consistency with the previous measurement.

$$j_k = \frac{jj_L}{j_L - j} \tag{9}$$

Therefore, it is justified that the NOR at Pd-GC electrode in neutral media containing 0.1 M KCl solution followed the first order kinetics.

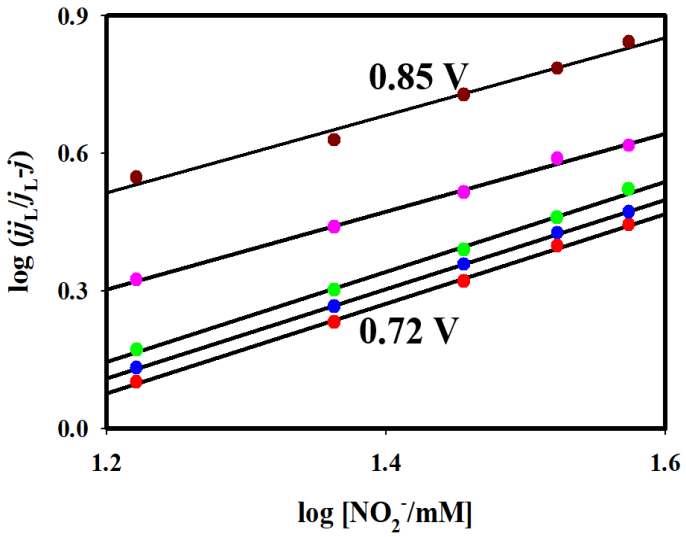

Fig. 13. Linear plot of log (jj_L/j_L-j) vs. log [NO_2^-/mM] for the order determination. Data were taken at (a) 0.72, (b) 0.75, (c) 0.77, (d) 0.80, (e) 0.85 V potential using **Fig 11.**

3.7. Koutecky–Levich (K–L) plots for the nitrite oxidation

Koutecky-Levich (K-L) is another significant tool in order to determine the kinectics of any electrochemical reaction. In the present case, we used *K-L* equation in order to rationalize the related kinetics as well as to determine the other kinetic parameters. *K-L* equation is expressed by equation (10)[45]

$$\frac{1}{j} = \frac{1}{j_k} + \frac{1}{B\omega^{1/2}} \qquad (10)$$

Where j_k is the kinetic current density equal to *nFCk*, *B* is regarded as *B* factor equal to $0.62\, nFAC_b D_0^{2/3} \upsilon^{-1/6}$ *k* is the rate constant and other symbols have their usual meaning. *B* can be determined by using equation (10) equal to the slope value of plot of j^{-1} vs $\omega^{-1/2}$ that should yield a straight line and intercept would be equal to j_k^{-1}. The values of *B* is also very helpful to determine the electrons number participated in the redox reaction and from the intercept one can easily estimate rate constant value. The values of j^{-1} were obtained from the Fig. 9. and plotted as a function of $\omega^{-1/2}$ represented in Fig 13 known as typical *K-L* plot. The linear and parallel of each lines in Fig. 14. reveals that the corresponding nitrite oxidation reaction was followed by first order kinetics under the influence of Pd-GC electrode that has a good agreement explained in the

previous section. The dotted line in the *K-L* plot represents as the theoretical line for *n=1* which clearly shows that the slope value of experimental line was very close to the theoretical line suggesting that only single electron transfer occurred in the nitrite oxidation reaction over the Pd-GC electrode. Different values of *n* were calculated from the slopes of the *K-L* plots and given in Table 1.

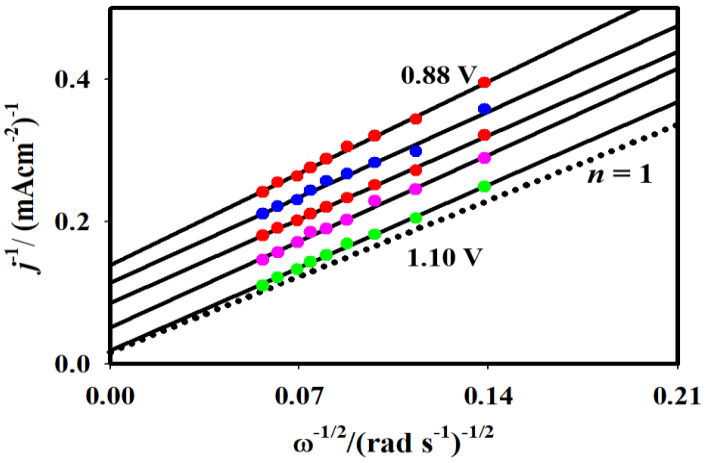

Fig 14. K-L plots for nitrite oxidation reaction over the Pd-GC electrode in 10 mM NaNO2 solution containing 0.1 M KCl. The specific plotential: (a) 0.884, (b) 0.934, (c) 0.953, (d) 0.975, (e) 1.10 V. The dotted line represent the experimental line for n=1.

Table 2. The value of obtained rate constant at different potential for the nitrite oxidation reaction at Pd-GC electrode containing 10 mM $NaNO_2$ in 0.1 M KCl.

E / V	0.88	0.93	0.95	0.97	1.0
n	0.97	1.01	0.98	0.98	1.00
$k \times 10^4$ / cms^{-1}	0.744	0.909	1.21	2.01	2.98

The kinetic current values or the rate constant were estimated at various potential from the intercepts of the *K-L* plots also represents in Table 2. The potential dependent rate constant can be defined by Equation (10) [43-45]

$$\ln(k) = \ln(k^0) + \frac{\beta nF}{RT}\eta \qquad (11)$$

Where η is the overpotential can be expressed as $\eta = E - E^0$ (E^0 is the standard electrode potential) and other symbols have usual meanings. k would be equal to k^0 if η =0, where k^0 is known as standard rate constant. The value of k^0 can be calculated from the plot of $\ln(k)$ vs η which should yield a straight line having an intercept equal to $\ln(k^0)$. A typical linear plot of $\ln(k)$ vs η was obtained and represented in Fig 15**.** The value of k^0 was calculated as $3.73 \times 10^{-7}\ cm\ s^{-1}$ considering the standard electrode potential (E^0) for the nitrite oxidation reaction in neutral media equal to 2.60×10^{-3} vs. Ag / AgCl / KCl (sat. KCl).

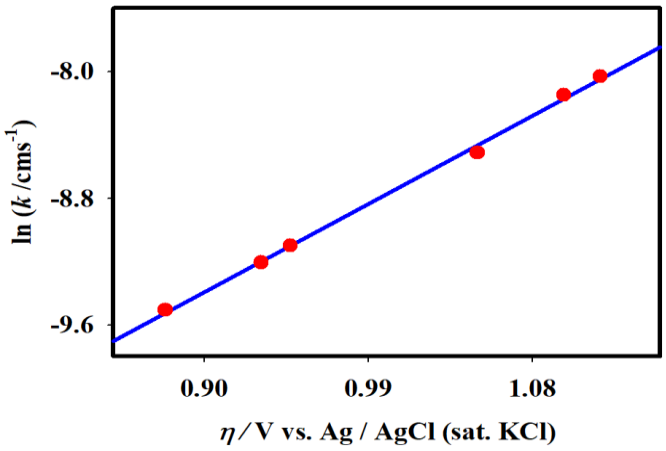

Fig. 15. Plot of ln (*k*) vs. η for the oxidation of nitrite in 0.1 m KCl at Pd-GC electrode.

3.8. Tafel plots

In order to further analysis of electro-kinetics, Tafel equation can play significant role from where one can predict the reaction mechanism and rate of the reaction. Tafel equation can be expressed by Equation (12) [45]

$$\eta = \frac{2.3RT}{n\beta F}\ log j_0 + \frac{2.3RT}{n\beta F} \log j \qquad (12)$$

Where η is the anodic overpotential and j_0 is the exchange current density and other symbols have their usual meanings. The relationship between overpotenital and logarithm of current density known as Tafel plot that should yield a straight line and from intercept of the straight line, exchange current density can be measured**.** Fig 16. represents a Tafel plot based on our present experiment at two different rotation rates specifically 2000 and 3000 rpm. The Tafel slope was found as 0.118V providing that overall reaction proceed followed by a single electron transfer process. The

exchange current density j_0 might be calculated if η is equal to zero. The values of j_0 might be changed depending on the nature of electrochemical reaction, reaction medium and influence of the supporting electrolyte [43, 45]. However, the values of j_0 for the nitrite oxidation reaction on Pd-GC electrode was determined as 1.6×10^{-8} mA cm^{-2} using the values of E^0 equal to 2.60×10^{-3} V vs. Ag / AgCl / KCl (sat. KCl).

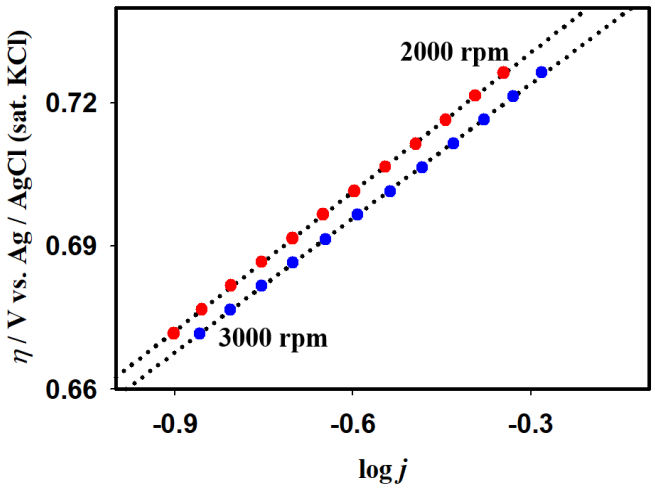

Fig 16. Tafel plot for nitrite oxidation at 2000 & 3000 rpm over Pd-GC electrode containing 10 mM $NaNO_2$ in 0.1 M KCl. Data were taken from Fig. 9.

4. Conclusion

The electrochemical nitrite oxidation reaction was investigated in presence of 10 mM $NaNO_2$ in 0.1 M KCl solution in neutral media using three different types (GC, Pd and Pd-GC) of electrodes. The electrolcatatlytic influence of Pd on GC enhance the performance of GC as Pd-GC electrode towards the oxidation of nitrite by lowering the oxidation potential (0.89V) with the increase of oxidation current. The extraordinary feature of Pd-GC electrode that it proceeds in nitrite oxidation following by the charge transfer process coupled with the homogenous chemical reaction as

$$NO_2^- \rightleftarrows NO_2 + e^-$$

$$2NO_2 + H_2O \rightarrow NO_2^- + NO_3^- + 2H^+$$

This mechanism having two steps was established through the cyclic and hydrodynamic voltammetric technique for the charge transfer process (first step) whereas the homogeneous chemical reaction as second step linked with the first step that produced the NO_3- was explored by

the bulk electrolysis techniques. The evidence of second step chemical reaction and kinetics of electron transfer reaction was ascertained in this present article. Involvement of number of electron in the charge transfer process was determined by the chronoamperometric technique suggested that only single electron transfer occurred in the nitrite oxidation reaction over the Pd-GC electrode that was furtherly proved by hydrodynamic voltammetry through the using of Levich and Koutechy – Levich equation. The charge transfer reaction order followed by a first order kinetics and the rate constant of this reaction varied from 0.744 to 2.98×10^{-4} cms^{-1} in the potential range of 0.88 V to 1.10 V. The standard rate constant (k^0) was calculated as $3.73 \times 10^{-7}\ cm\ s^{-1}$ for the corresponding charge transfer reaction. The Tafel slope of 0.118 V was obtained indicating that single electron involved in the rate determining step.

5. References

[1] A.J. Dumham, R.M. Barkley, R.E. Sievers. Anal. Chem., 67 (1995) 220.

[2] X.H. Chen, C.M. Ruan, J.L. Kong, J.Q. Deng. Anal. Chim. Acta, 382 (1999) 189.

[3] A.E. Williams, J.A. Johnson, L.J. Lund, Z.J. Kabala. J. Environ. Qual., 27(1998) 1147.

[4] Denshaw-Burke, Mary (2006-11-07). "Methemoglobinema". Retrieved 2008-03-31.

[5] D. M. Manassaram, L. C. Backer, R. Messing, L. E. Fleming, B. Luke, C. P. Monteilh, Environmental Health. 9 (2010) 60.

[6] M. Parvizishad, A. Dalvand, A. H. Mahvi, F. Goodarzi, Health Scope: 6 (2017) 3.

[7] K. Suvardhana, K.S. Kumara, S.H. Babua, B. Jayarajb, P. Chiranjeevia. Talanta, 66 (2005) 505.

[8] M.N. Abbas, G.A. Mostafa. Anal. Chim. Acta, 410 (2000) 185.

[9] X. Zhang, H. Wang, N.N. Fu, H.S. Zhan. Spectrochim. Acta A, 59 (2003) 1667.

[10] M.T. Fernandez-Arguelles, B. Canabate, J.M. Costa-Fernandez, R. Pereiro, A. Sanz-Medel. Talanta, 62 (2004) 991.

[11] V. Jedlickova, Z. Paluch, S. Alus|k. J. Chromatogr. B, 780 (2002)193

[12] S. Bilal Butt, M. Riaz, M. Zafar Iqbal. Talanta, 55 (2001) 789.

[13] D. Tsikas, S. Rossa, J. Sandmann, J.C. Frolich. J. Chromatogr. B, 724 (1999)199.

[14] J. Lee, E. Ban, Seh-Yoon Yi, Young Sook Yoo. J. Chromatogr. A, 1014 (2003) 189.

[15] J.E. Melanson, C.A. Lucy. J. Chromatogr. A, 884(2000) 311.

[16] C. Lua, J.M. Lin, C.W. Huie, M. Yamada. Anal. Chim. Acta, 510 (2004) 29.

[17] L.Y. Jiang, R.X. Wang, X.M. Li, L.P. Jiang, G.H. Lu. Electrochem. Commun., 7 (2005) 597.

[18] M.H. Pournaghi-Azar, H. Dastangoo. J. Electroanal. Chem., 567 (2004) 211.

[19] J.R. Rocha, L. Kosminsky, T.R.L.C. Paixao, M. Bertotti, Electroanalysis 13 (2001) 155.

[20] R. Guidelli, F. Pergola, G. Raspi, Anal. Chem., 44, (1972) 745.

[21] B. Piela, P. K. Wrona, J. Electrochem. Soc. 149 (2002) 55-63.

[22] X. Zhu, G. Kang, X. Lin, Microchim. Acta 159 (2007) 141–148.

[23] P. Muthukumar, S. Abraham John, J. Colloid Interface Sci. 421 (2014) 78–84.

[24] Y. Liu, J. Zhou, J. Gong, W.-P. Wu, N. Bao, Z.-Q. Pan, J. Electrochim. Acta 111 (2013) 876–887.

[25] L. Lu, S. Wang, T. Kang, W. Xu, Microchim. Acta 162 (2007) 81–85.

[26] J. Lin, C. He, Y. Zhao, S. Zhang, Sensors Actuators B: Chem. 137 (2009) 768–773.

[27] K. Zhao, H. Song, S. Zhuang, L. Dai, P. He , Y. Fang, Electrochem Commun 9 (2007) 65–70.

[28] Y. Wang, E. Laborda, R. G. Compton, Journal of Electroanalytical Chemistry, 670 (2012) 56-61.

[29] Claudia A Caro, Fethi Bedioui, J. H. Zagal, Electrochimica Acta Volume 47, Issue 9, 15 February 2002, Pages 1489-1494]

[30] J. Kariuki, E. Ervin, C. Olafson, *Sensors* 15 (2015)18887-18900.

[31] J. Yang. H. Yang, S. Liu, L. Mao, Sensors and Actuators B; Chemical 220 (2015) 652-658

[32] Y. Zhang, Y. Zhao, S. Yuan, H. Wang, C. He, s*ensors and Actuators B: Chemical* (2013), DOI: http://dx.doi.org/doi:10.1016/j.snb.2013.05.059

[33] M. Peuckert, *J. Phys. Chem.*, 89 (12) (1985) 2481–2486

[34] A. Gniewek, J. catal 229 (2005) 332-343.

[35] W. J. Plieth, Diplomarbeit, Freie Universitat Berlin 1961

[36] Yu. I. Erlikh, K. L. Anni, and U. V. Palm, Elektrokhimiya, 14 (1978) 1066.

[37] Y. N. Jiang, H. Q. Luo, N. B. Li, Intern. J. Environ. Anal. Chem. 87 (2007) 295–306.

[38] J. Yang. H. Yang, S. Liu, L. Mao, Sensors and Actuators B; Chemical 220 (2015) 652-658

[39] M.A. Hasnat, M.A. Rashed, M. S. Alam, M. M. Rahman, M. A. Islam, S. Hossain, N. Ahmed, Catal. Commun. 11 (2010) 1085–1089

[40] M. A. Bhat, P. P. Ingole, V. R. Chaudhari, S. K. Haram, New. J. Chem, 33 (2009) 207-210.

[41] M. A. Bhat, P. P. Ingole, V. R. Chaudhari, S. K. Haram, J. Phys. Chem., 113 (2009) 2848-2853.

[42] N. Tanjila, A. Rayhan, M. S. Alam, I. A. Siddiquey, M. A. Hasnat, RSC Adv., 6, 2016, 93162–93168.

[43] C.-C. Chang, T.-C.Wen, H.-J. Tien, Electrochim. Acta 42 (1997) 557.

[44] M. S. Alam, M.A. Hasnat, M.A. Rashed, M. R. Miah, I. S.M. Saiful, Electrochim. Acta 76 (2012) 102– 105

[45] A.J. Bard, L.R. Faulkner, Electrochemical Methods: Fundamental and applications, John Wiley and Sons, Inc, New York, 2001 (Chapters 1, 3 and 9).